

ARTICLE



GTSE1 promotes tumor growth and metastasis by attenuating of KLF4 expression in clear cell renal cell carcinoma

Weihao Chen^{1,2,5}, Hanfeng Wang^{1,5}, Yongliang Lu^{1,2,5}, Yan Huang¹, Yundong Xuan^{1,2}, Xiubin Li¹, Tao Guo^{2,3}, Chenfeng Wang^{1,2}, Dong Lai¹, Shengpan Wu¹, Wenlei Zhao², Haixing Mai^{1,4}, Hongzhao Li¹, Baojun Wang¹, Xin Ma¹ and Xu Zhang¹

© The Author(s), under exclusive licence to United States and Canadian Academy of Pathology 2022

Clear cell renal cell carcinoma (ccRCC) is one of the most common malignant tumors and is characterized by a poor prognosis. Although G2- and S-phase expressed-1 (GTSE1) is known to be involved in the progression and metastasis of various cancers, its significance and mechanism in ccRCC remain unknown. In the present study, we found that GTSE1 was overexpressed in ccRCC tissues, especially in metastatic samples. Moreover, high GTSE1 expression was positively correlated with higher pT stage, tumor size, clinical stage, and WHO/ISUP grade and worse prognosis. And GTSE1 expression served as an independent prognostic factor for overall survival (OS). In addition, GTSE1 knockdown inhibited ccRCC cell proliferation, migration, and invasion, and enhanced cell apoptosis in vitro and in vivo. GTSE1 was crucial for epithelial–mesenchymal transition (EMT) in ccRCC. Mechanistically, GTSE1 depletion could upregulate the expression of Krüppel-like factor 4 (KLF4), which acts as a tumor suppressor in ccRCC. Downregulation of KLF4 effectively rescued the inhibitory effect induced by GTSE1 knockdown and reversed the EMT process. Overall, our results revealed that GTSE1 served as an oncogene regulating EMT through KLF4 in ccRCC, and that GTSE1 could also serve as a novel prognostic biomarker and may represent a promising therapeutic target for ccRCC.

Laboratory Investigation (2022) 102:1011–1022; <https://doi.org/10.1038/s41374-022-00797-5>

INTRODUCTION

Renal cell carcinoma (RCC) is one of the most frequently occurring malignant tumors of the urinary system¹. Clear cell RCC (ccRCC) is a major pathological type of RCC, accounting for approximately 75% of all RCC cases^{2,3}. Although nephrectomy shows curative potential for most localized cases of ccRCC, up to one-third of patients will develop metastasis, which remains the main reason for disease progression^{2,4}. The prognosis of advanced ccRCC is poor due to its heterogeneity and its intrinsic resistance to traditional chemotherapy and radiotherapy⁵. However, the emergence of systemic methods for ccRCC treatment, including the use of vascular endothelial growth factor (VEGF) receptor, tyrosine kinase inhibitors, the mammalian target of rapamycin (mTOR) pathway inhibitors, and immune checkpoint inhibitors, have improved the outcomes for patients⁴. Unfortunately, patients with advanced-stage disease frequently experience severe drug side effects and drug resistance, and most ccRCC patients do not show durable clinical benefit^{6,7}. Therefore, investigations of the molecular mechanism of ccRCC progression and metastasis with the aim of providing a molecular basis and developing therapeutic targets for this condition have gained in importance.

G2 and S phase-expressed-1 (GTSE1) protein is a cell cycle-related protein co-localized in microtubules and tubulin, which has been found to be expressed specifically in the G2 and S phases of the cell cycle⁸. GTSE1 is also a key regulator of the chromosome alignment and spindle pole integrity. This is done by

regulating the dynamics of microtubules during mitosis⁹. In addition, GTSE1 regulates P53 negatively by transporting it to the cytoplasm for further degradation^{10,11}. Previous studies have shown that GTSE1 plays an oncogene role to promote cell proliferation, migration and invasion, and serves as a biomarker for poor clinical outcome in many solid tumors^{12–14}. However, up until now, the expression and biological function of GTSE1 in ccRCC remained unknown.

In the present study, we aimed to investigate the clinical significance and function of GTSE1 in ccRCC. Surprisingly, we found that GTSE1 mRNA and protein levels were higher in the ccRCC tissues and cell lines, and high GTSE1 levels were positively correlated with poor outcomes in ccRCC patients. Subsequently, GTSE1 knockdown significantly inhibited the proliferation, migration, and invasion of ccRCC and induced cell apoptosis in ccRCC cells. In addition, downregulation of GTSE1 was shown to disrupt epithelial-to-mesenchymal transition (EMT). Further studies showed that GTSE1 plays the role of an oncogene by regulating KLF4 expression. Collectively, our results indicated that GTSE1 might exert a tumor-promoting effect on ccRCC.

MATERIALS AND METHODS

Patients and tissue specimens

From August 2012 to November 2017 tissue microarrays containing 199 ccRCC tissues and 115 adjacent normal renal tissues, were constructed in

¹Department of Urology, the Third Medical Center, Chinese PLA General Hospital, Beijing 100039, China. ²Medical School of Chinese PLA, Beijing 100853, China. ³Department of Paediatrics, the Seventh Medical Center, Chinese PLA General Hospital, Beijing 100700, China. ⁴The Second School of Clinical Medicine, Southern Medical University, Guangzhou 510280, China. ⁵These authors contributed equally: Weihao Chen, Hanfeng Wang, Yongliang Lu. ✉email: baojun40009@126.com; urologist@foxmail.com; xzhang301@163.com

Received: 4 January 2022 Revised: 29 March 2022 Accepted: 18 April 2022

Published online: 18 May 2022

our laboratory. Data for clinicopathological features such as sex, age, body mass index (BMI), tumor size, TNM stage (TNM Classification of Malignant Tumors), WHO/ISUP grade, and outpatient follow-up data were reviewed and extracted from medical records and outpatient follow-up examinations. Informed consent was obtained from all patients. The study was approved by the Ethics Committee of PLA General Hospital. The pathological diagnoses were confirmed by two senior pathologists according to 2016 WHO Classification of Tumors of the Urinary System and Male Genital Organs², and clinical staging was performed on the basis of the eighth American Joint Committee on Cancer TNM staging system¹⁵.

Cell lines and culture conditions

The human renal proximal tubular epithelial cell lines, the human kidney epithelial cell (HKC) and HK2, and the human ccRCC cell lines 786-O, A498, 769-P, Caki-1, OSRC-2, SN12-PM6, and HEK293T were preserved in our laboratory. A498, 786-O, Caki-1, Caki-2, OSRC-2 and SN12-PM6 cells were cultured in minimum essential medium (MEM), RPMI 1640, McCoy's 5 A, and Dulbecco's modified Eagle medium (DMEM; Gibco), all of which were supplemented with 10% fetal bovine serum (FBS) (Invitrogen) and 1% penicillin–streptomycin. All cells were incubated at 37 °C with 5% CO₂ under mycoplasma-free conditions.

Generation of knockdown cell lines

Short hairpin RNA (shRNA) against the human GTSE1 was designed and synthesized (Invitrogen). The target sequences for sh-GTSE1-1 and sh-GTSE1-2 for humans were 5'-CCGGGCTACTCTACAATCAATTCGAG AATTGATTTGTAGGAGTAGGCTTTTGG-3'; 5'-CCGGGCCAGCTTGAATTAAT AATCTCGAGATTATTAATTCAGCTGGCTTTTGG-3'. The corresponding double-stranded oligonucleotides were inserted into the pLKO vector digested with AgeI and EcoRI to construct the pLKO-shGTSE1 plasmid. A lentivirus was produced as described previously¹⁶. To generate stable shRNA knockdown cells, targeted ccRCC cells were transfected with lentivirus in the presence of polybrene (2 µg/mL, Millipore) for 24 h. After puromycin (2 µg/mL, Sigma) selection for 48 h, single-cell clones were expanded, the gene disruption was validated by quantitative reverse transcription-polymerase chain reaction (qRT-PCR) and western blot analysis.

Small interfering RNA (siRNAs) targeting KLF4 were designed and synthesized (Invitrogen). The sequence of si-KLF4 was 5'-GCACUACAAU-CAUGGUCAATT-3'; 5'-UUGACCAUGAUUGUAGUGCTT-3'. A non-targeting siRNA (si-CTRL) was used as the negative control. Cells were transfected using Lipofectamine RNAi-MAX (Invitrogen) mixed with 10 nmol/L siRNA.

Western blotting

Western blotting was performed using a standard protocol. Briefly, cells were lysed in radioimmunoprecipitation assay (RIPA) buffer (Thermo Scientific) supplemented with a complete protease inhibitor (Roche) and phosphatase inhibitor cocktail (Thermo Scientific) for 30 min on ice, which was followed by pelleting of insoluble material by centrifugation. Lysates were heated to 95 °C in sodium dodecyl sulfate (SDS) sample buffer for 10 min, separated by SDS-polyacrylamide gel electrophoresis (PAGE), and subsequently transferred to polyvinylidene difluoride (PVDF) membranes (Millipore, Billerica, MA). The membranes were blocked in 5% non-fat milk for 1 h at 37 °C, and then incubated with primary antibodies overnight at 4 °C. After three washes in TBST buffer, the membranes were incubated with the corresponding horseradish peroxidase (HRP)-conjugated anti-mouse or anti-rabbit secondary antibodies (ZSGB-BIO, Beijing, China), for 2 h at room temperature. The signals of the target proteins were visualized using an enhanced chemiluminescence detection kit (Thermo, IL) and analyzed with the ChemiDoc System (Bio-rad, USA). The primary antibodies included Rabbit anti-GTSE1 (Proteintech; 21319-1-AP), rabbit anti-KLF4 (Proteintech; 11880-1-AP), rabbit anti-BCL2 (Proteintech; 12789-1-AP), rabbit anti-cleaved caspase-3 (Cell Signaling Technology; #9664), rabbit anti-E-cadherin (Proteintech; 20874-1-AP), rabbit anti-N-cadherin (Proteintech; 22018-1-AP), rabbit anti-Snail (Proteintech; 13099-1-AP), rabbit anti-vimentin (Proteintech; 10366-1-AP), rabbit anti-Twist1 (Proteintech; 25465-1-AP), rabbit anti-CD44 (Proteintech; 15675-1-AP), rabbit anti-MMP2 (Proteintech; 10373-2-AP) and rabbit anti-MMP9 (Proteintech; 10375-2-AP).

Quantitative reverse transcription-polymerase chain reaction (RT-qPCR)

The total RNA was isolated using Trizol reagent (Invitrogen) for purification with PARISTM Kit (Applied Biosystems) according to the manufacturer's protocol, which was then used for reverse transcription with a cDNA

Synthesis Kit (TransGen Biotech). RT-qPCR was conducted using SYBR Green qPCR reagent (TransGen Biotech) with peptidylprolyl isomerase A (PPIA) serving as the internal control. Relative expression was normalized to PPIA and calculated as $2^{-[\text{CT of candidate genes} - (\text{CT of PPIA})]}$. The primer for GTSE1 sequences was 5'-CGCTTGGTTCAGAAATCTTC-3', 5'-TGTAGGAGTAGGC ATAACC-3'. The primer for PPIA sequences was 5'-ATGGTCAACCCC ACCGTGT-3', 5'-TCTGCTGCTTTGGACCTTGTC-3'.

Immunohistochemistry (IHC)

For all human tissues and xenograft tumor tissues, immunohistochemistry (IHC) was performed as described previously^{17,18}. The primary antibodies included Rabbit anti-GTSE1 (Proteintech; 21319-1-AP), and rabbit anti-Ki-67 (Cell Signaling Technology; #9129). The IHC scoring was performed independently by three experienced pathologists. The percentage of positive cells was classified as follows: <10% = 0, 11%–25% = 1, 26%–50% = 2, 51%–75% = 3, and >75% = 4. The staining intensity was classified as follows: no staining = 0, weak intensity = 1, moderate-intensity = 2, and strong intensity = 3. The final IHC score was calculated by multiplying the staining intensity and the proportions of stained cells. Finally, tissues with scores ≥ 6 were defined as showing high expression, whereas the others were defined as showing low expression.

Cell-proliferation and apoptosis assays

For cell-proliferation assays, cells were seeded onto a 6-well plate, infected with lentiviral particles, and cultured for 96 h, and the proliferation index for cells was calculated and plotted. The MTS assay was also performed according to the manufacturer's protocols to examine the cell-proliferation ability. In brief, cells stably expressing control shRNA or shGTSE1 were seeded in 96-well plates and absorbance was measured at the time points of 0, 1, 2, 3, 4, 5, and 6 days after seeding. All experiments were performed in triplicate.

For the apoptosis assay, an Annexin V-FITC apoptosis detection kit (Beyotime) was used according to the manufacturer's protocol. In brief, cells were harvested and resuspended in binding buffer to prepare single-cell suspensions and incubated with annexin V-FITC/PI in the dark for 30 min. Then, the stained cells were analyzed by flow cytometry using FloMax software. All experiments were performed in triplicate.

Wound-healing assay

Cells were seeded in a 6-well plate and cultured in serum-free medium. Pictures of wounds were taken at 0 and 24 h after scratching with a sterile 200 µL pipette tip. The percentage of the wound closure area was measured at three different positions. All experiments were performed in triplicate.

Migration and invasion assay

Cells were seeded into an upper transwell chamber (8 µm, Corning), which was coated with 20 µL of Matrigel (Corning) before cell seeding for the invasion assay. After incubation, the chamber membranes were fixed with 4% paraformaldehyde and stained with 1% crystal violet for 15 min, and the number of migrated or invaded cells was analyzed by calculating six random fields. All experiments were conducted at least three times.

Mouse xenograft renal cancer model

All animal studies were approved by the Medical Experimental Animal Care Commission of PLA General Hospital. Four-week-old BALB/c nude mice were purchased from Vital River (Beijing) and maintained under specific pathogen-free conditions. SN12-PM6 cells with stable GTSE1 knockdown and control vector (1×10^7 cells/100 µL in a 1:1 solution of PBS/Matrigel) were orthotopically injected into the right kidney of nude mice (5 mice per group). All mice were sacrificed four weeks after implantation, and tumor weight and lung metastatic nodules were measured.

Statistical analyses

All experiments were performed in triplicate. Data were presented as means ± standard deviation (SD). All statistical analyses were performed using SPSS 22.0 (SPSS Inc., USA). For comparisons, Student's *t*-test, the Chi-square (χ^2) test, and one-way analysis of variance (ANOVA) were applied as appropriate. The Kaplan–Meier method was used to analyze survival curves, and the log-rank test was used to assess the differences in survival. Spearman's correlation test was performed to analyze the correlations between the variables. Independent prognostic factors were identified

using univariate and multivariable Cox regression analyses, and p values < 0.05 indicated statistical significance.

RESULTS

The GTSE1 mRNA expression pattern and its significance for ccRCC in TCGA

To assess the role of GTSE1 in the development of ccRCC, we first evaluated the mRNA expression level of GTSE1 in the TCGA database. As shown in Fig. 1A, GTSE1 was significantly overexpressed in ccRCC in comparison with normal kidney tissue. In addition, high GTSE1 mRNA expression was markedly associated with advanced TNM stages (Fig. 1B–D), pathology histologic grade (Fig. 1E), and the clinical stage (Fig. 1F) of the TCGA database of patients.

To evaluate whether the expression levels of GTSE1 were associated with the prognosis in ccRCC patients, the ccRCC patients in the TCGA database were divided into two groups: namely, the GTSE1 high-expression group and the GTSE1 low expression group. The Kaplan–Meier analysis indicated that the patients in the GTSE1 high-expression group had worse OS (Fig. 1G) and a shorter disease-free survival rate (Fig. 1H). Further, univariate Cox proportional hazards regression analysis showed that in advanced TNM stage, pathological grade, clinical stage, and high GTSE1 expression were correlated with poorer OS (Fig. 1I). In addition, the multivariable Cox regression analysis showed that GTSE1 expression along with tumor metastasis, advanced pathological grade, and clinical stage were independent prognostic factors for ccRCC patients (Fig. 1J). Collectively, these data suggested that GTSE1 plays an important role in the malignant progression of ccRCC.

GTSE1 is upregulated in ccRCC and predicts poor clinical outcomes

To validate the results in the TCGA database, we analyzed both the mRNA and the protein levels in a cohort of clinical tissues by using qRT-PCR and western blotting. Both the GTSE1 mRNA and protein levels showed consistent and significant upregulation in ccRCC tissues in comparison with those in adjacent normal tissues (Fig. 2A, B). In addition, we also measured the mRNA and protein expression levels of GTSE1 in ccRCC cell lines (786-O, A498, 769-P, Caki-1, OSRC-2, SN12-PM6) and normal human kidney epithelial cell lines (HKC, HK2). As shown in Fig. 2C, D, in comparison with the normal renal cell lines HKC and HK2, the ccRCC cell lines showed notably increased GTSE1 mRNA and protein expression levels.

To further identify the GTSE1 protein expression level and location in ccRCC tissues, we performed immunohistochemical analysis by tissue microarrays (TMAs) including 199 ccRCC tissues and 115 normal renal tissues. The results showed that GTSE1 was predominantly located in the cytoplasm of tumor cells, and its protein expression was obviously higher than that in ccRCC tissues (Fig. 2E, F). Consistent with the results from the TCGA database, GTSE1 expression was increased in the advanced clinical stages (Fig. 2G), especially in ccRCC patients with preoperative lymphatic metastasis and distant metastasis (Fig. 2H, I). The correlations between GTSE1 expression and the clinical pathological characteristics are shown in Table 1. GTSE1 expression was not associated with patient age, sex, and BMI. GTSE1 overexpression was strikingly correlated with tumor size ($p = 0.0023$), pT stage ($p = 0.0034$), clinical stage ($p = 0.0008$), WHO/ISUP grade ($p = 0.0006$), and metastasis status ($p = 0.021$).

Subsequently, Kaplan–Meier analyses with a log-rank test for overall survival (OS) and disease-free survival (DFS) were performed to elucidate the relationship between GTSE1 expression in TMA and patient survival in 199 ccRCC patients. Our results revealed that high expression of GTSE1 was associated with the poor OS and a shorter Disease free survival rate (DFS) in comparison with lower GTSE1 expression (Fig. 2J, K, $p < 0.001$). In addition, further OS analysis was performed on the basis of the tumor clinical stage,

and the results suggested that patients with stage I-II or stage III-IV disease and higher GTSE1 expression had a worse prognosis than those with lower GTSE1 expression (Fig. 2L, M).

Further, univariate analysis showed that pT stage, tumor size, clinical stage, WHO/ISUP grade, lymph node invasion, distant metastasis, and GTSE1 protein expression were predictive of poor outcomes. In the Cox multivariable analysis, GTSE1 protein expression, WHO/ISUP grade, and distant metastasis status were found to be the strongest individual clinical factors (Table 2).

Taken together, the TCGA data and our clinical data suggest that GTSE1 upregulation may lead to ccRCC malignant progression and may represent a useful prognostic marker for ccRCC.

GTSE1 knockdown inhibited cell proliferation and induced apoptosis in vitro

Based on our finding that GTSE1 expression is correlated with ccRCC prognosis, we next investigated the function of GTSE1 in ccRCC cells. We initially evaluated the correlation between GTSE1 expression level and the expression of Ki-67, a marker that is strongly associated with tumor cell proliferation and growth¹⁹. As expected, GTSE1 expression was significantly positively correlated with Ki-67 expression in ccRCC tumors from the TCGA database (Fig. 3A). To further investigate the effect of GTSE1 on ccRCC growth, GTSE1 was depleted by shRNA in ccRCC cells, and the knockdown efficiency was assessed by western blotting (Fig. 3B, C). In comparison with the negative control, GTSE1 silencing notably inhibited the cell-proliferation abilities in both 786-O and Caki-1 cells (Fig. 3D–G).

In addition, we investigated the effects of GTSE1 on ccRCC apoptosis induction by flow cytometry. The results showed that the percentage of apoptotic cells dramatically increased in 786-O and Caki-1 cells transfected with shGTSE1-1 and shGTSE1-2 in comparison with the cells transfected with the control shRNA group (Fig. 3H, I). The corresponding western blotting results showed increased expression of cleaved caspase-3 and significantly decreased expression of Bcl-2 in both 786-O and Caki-1 cells after silencing GTSE1 (Fig. 3J, K).

GTSE1 depletion impairs ccRCC cell migration and invasion in vitro

To investigate whether suppression of GTSE1 could alter ccRCC cells' migratory and invasive abilities, we conducted wound-healing and transwell assays. As shown in Fig. 4A, in the wound-healing assay, knockdown of GTSE1 expression in 786-O and Caki-1 cells significantly suppressed cell migration ability in comparison with that in the control shRNA group. Transwell assays also confirmed that downregulated GTSE1 expression markedly reduced the migratory and invasive capacities in ccRCC cell lines (Fig. 4B, C).

Acquisition of the epithelial–mesenchymal transition (EMT) phenotype is known to be a critical process for epithelial cells to gain the capacity to migrate and invade. Further, tumor cells that undergo an EMT acquire cancer stem-cell like properties and show an increase in CD44 expression²⁰. Recent studies have reported that GTSE1 promotes EMT progression in various tumors^{14,21}. Therefore, we also examined the expression of EMT-related proteins and CD44 protein by western blotting. Inhibition of GTSE1 expression increased the levels of E-cadherin, and decreased the N-cadherin, vimentin, Twist1, Snail, MMP2 and MMP9 levels, suggesting that GTSE1 is a driver of EMT in ccRCC (Fig. 4D, E). However, no significant change was noted in the CD44 expression in the GTSE1 knockdown groups (Supplementary Fig. 1). Thus, our in vitro data showed that GTSE1 plays a promoting role in the regulation of migration and invasion in ccRCC cells.

GTSE1 knockdown suppresses tumor growth and metastasis in vivo

Since GTSE1 silencing impaired the proliferation, migration, and invasion of ccRCC cells in vitro, we next explored whether GTSE1 plays a role in ccRCC growth and metastasis in vivo. Kidney

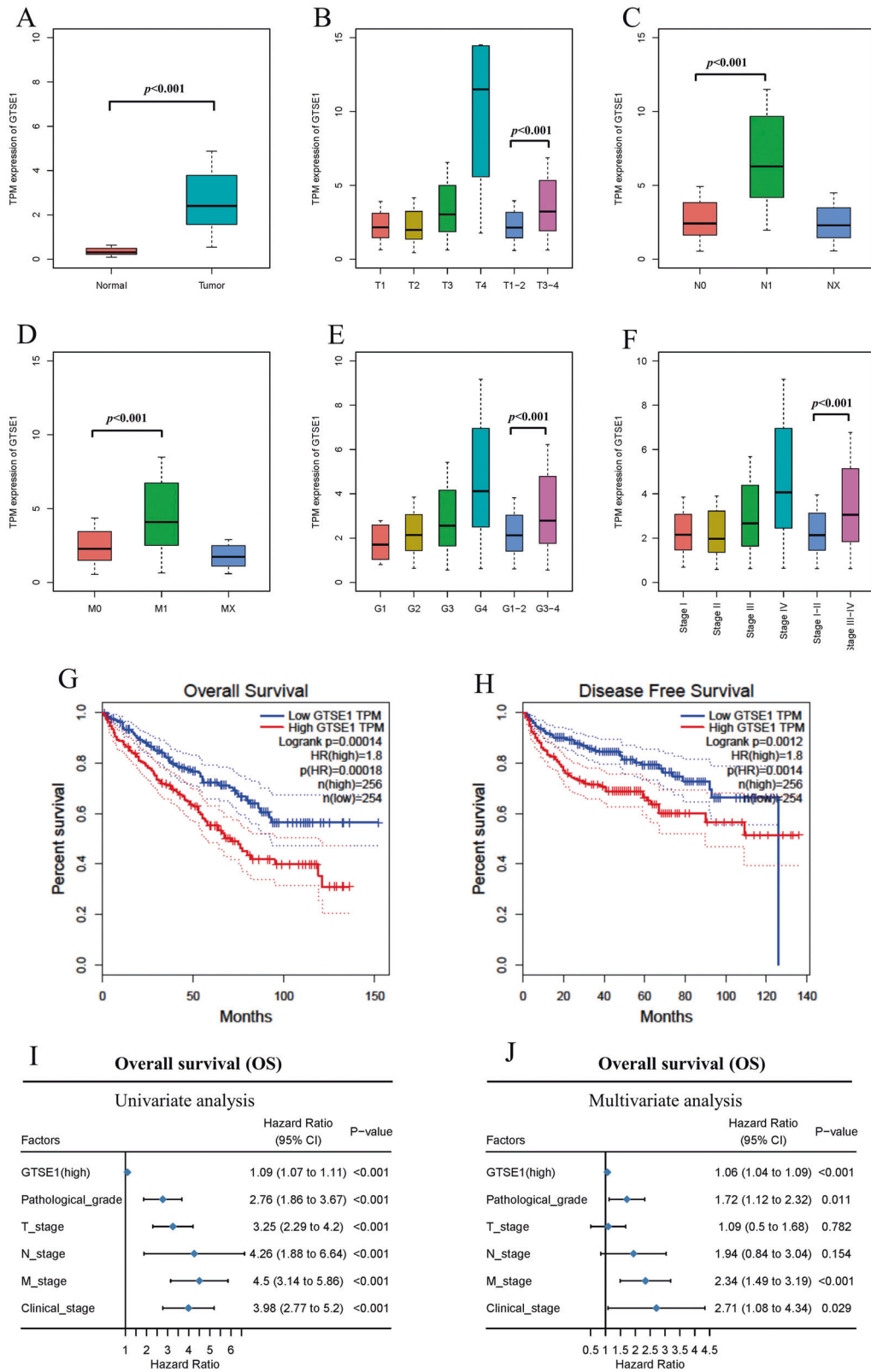


Fig. 1 The GTSE1 mRNA expression pattern and significance for ccRCC in TCGA. **A**. The expression of GTSE1 in ccRCC from TCGA. The expression of G2- and S-phase expressed-protein 1 (GTSE1) in different stages and grades: tumor T stage (**B**), lymphatic invasion (**C**), metastasis status (**D**), pathology histologic grade (**E**), clinical stage (**F**). Kaplan-Meier analysis indicated that higher expression of GTSE1 was associated with shorter overall survival (**G**) and disease-free survival (**H**). The outcome of univariate (**I**) and multivariable analysis (**J**). The Hazard Ratios (HRs) are presented as the means (95% confidence interval). Error bars represent Standard Deviation of the mean. (Student's *t*-test, one-way ANOVA).

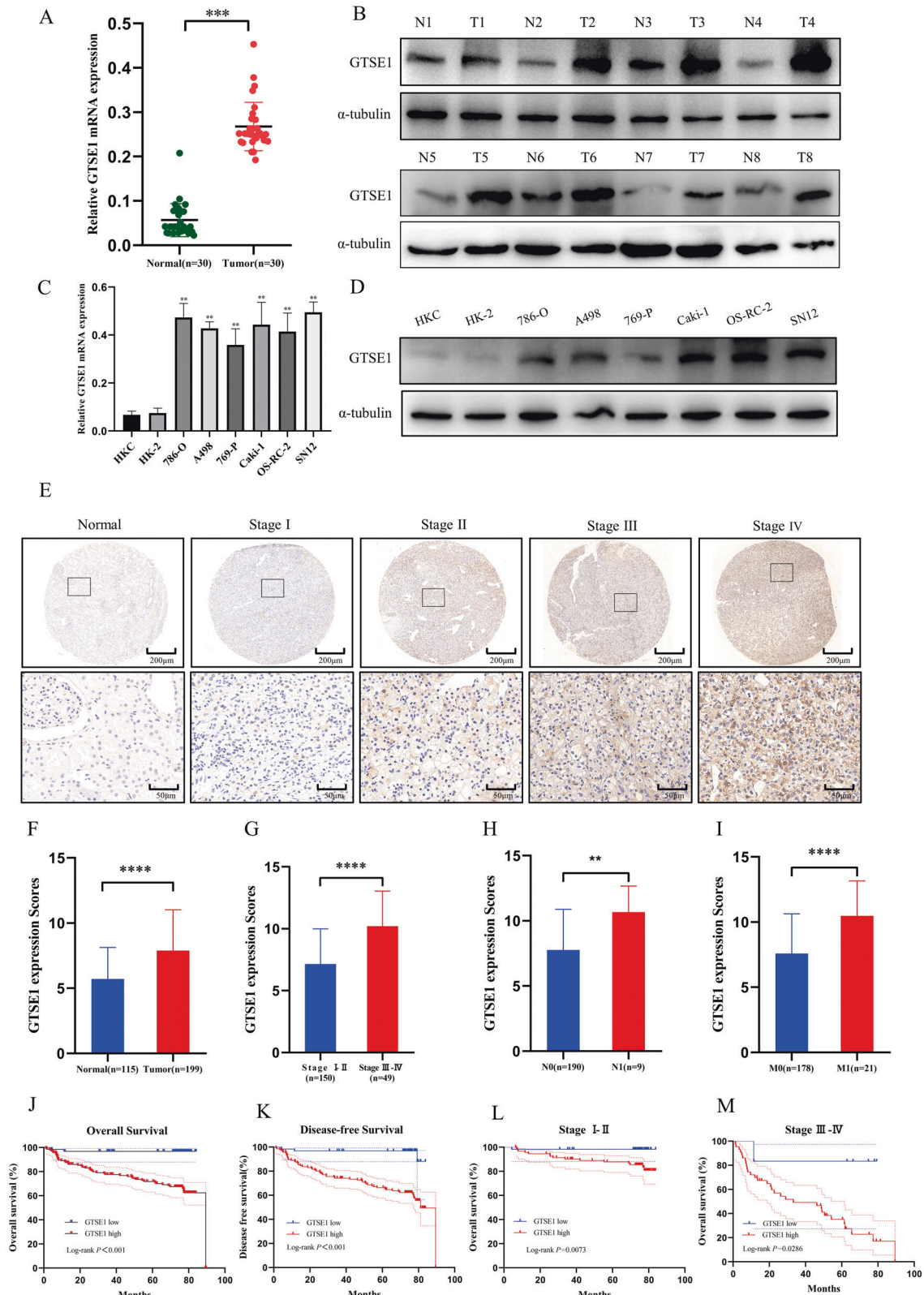


Fig. 2 GTSE1 is upregulated in ccRCC and predicts poor clinical outcomes. qRT-PCR (A) and Western blot (B) analysis of GTSE1 expression levels in ccRCC tissues and paired adjacent normal tissues. Real-time quantitative polymerase chain reaction (qRT-PCR) (C) and Western blot (D) analysis of GTSE1 expression levels in ccRCC cell lines and normal human kidney epithelial cell lines. Representative Tissue micro-array (TMA) images show GTSE1 staining (E), and comparison of the Immuno-histochemistry (IHC) score between tumor and non-tumor renal tissues (F). The expression of GTSE1 in different clinical stages and metastasis status: clinical stage (G), lymphatic metastasis (H) and distant metastasis (I). J, K OS and DFS curve of TMA patients based on GTSE1 expression according to Kaplan-Meier analysis. OS curve (J), DFS curve (K). L, M OS curve of TMA patients with different GTSE1 expression was further analyzed according to clinical stage, stage I,II (L) or stage III,IV (M). The n values indicate the number of patients. Error bars represent SD of the mean. ** $p < 0.01$, *** $p < 0.001$, **** $p < 0.0001$.

Table 1. The Correlation between GTSE1 expression and clinicopathological parameters of ccRCC patients.

Variables	No. of patients (n = 199)	Low expression	High expression	P value
Age				
≤56	104	34	70	0.7428
>56	95	29	66	
Sex				
Male	137	39	98	0.150
Female	62	24	38	
BMI(kg/m ²)				
≤25	116	42	74	0.1029
>25	83	21	62	
Tumor size(cm)				
≤7	166	60	106	0.0023 ^a
>7	33	3	30	
pT stage				
T1 + T2	163	59	104	0.0034 ^a
T3 + T4	36	4	32	
Clinical stage				
I,II	150	57	93	0.0008 ^a
III,IV	49	6	43	
WHO/ISUP grade				
1–2	127	51	76	0.0006 ^a
3–4	72	12	60	
Metastasis				
No	178	61	117	0.0211 ^a
Yes	21	2	19	

^aStatistically significant ($p < 0.05$).
 p value from Chi-square test.

Table 2. Univariate and multivariate cox proportional regression analysis with overall survival.

Variable	Univariate analysis			Multivariate analysis		
	HR	95%CI	P value	HR	95%CI	P value
Age						
≤56 vs >56	1.179	0.6653–2.089	0.573			
GTSE1 expression						
Low vs High	1.604	1.392–1.849	<0.001 ^a	1.337	1.1508–1.553	<0.001 ^a
Tumor size(cm)						
≤7 vs >7	5.173	2.885–9.276	<0.001 ^a	0.857	0.4276–1.717	0.663463
pT stage						
T1-T2 vs T3-T4	5.794	3.237–10.37	<0.001 ^a	1.896	0.6188–5.809	0.26276
Clinical stage						
I-II vs III-IV	10.21	5.513–18.92	<0.001 ^a	1.185	0.3226–4.350	0.798532
WHO/ISUP grade						
1–2 vs 3–4	15.07	6.725–33.78	<0.001 ^a	4.584	1.7724–11.858	0.00168 ^a
Lymph node invasion						
N0 vs N1	4.385	1.711–11.24	0.00208 ^a	1.296	0.6188–5.809	0.637149
Metastasis						
M0 vs M1	9.677	5.19–8.04	<0.001 ^a	3.022	1.126–8.11	0.02812 ^a

CI confidence interval, HR hazard ratio.

^aStatistically significant ($p < 0.05$).

p value from Cox regression analyses.

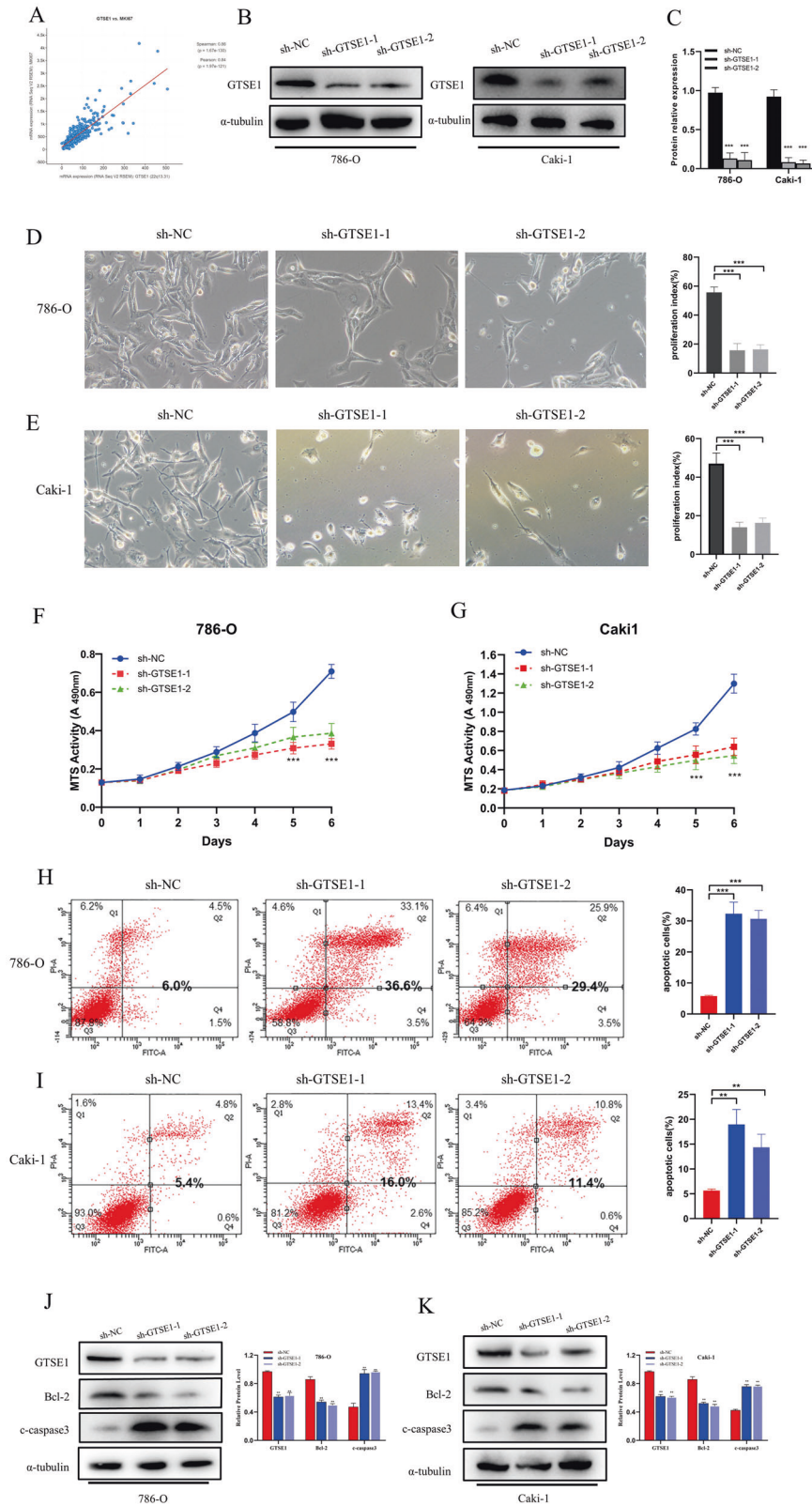


Fig. 3 GTSE1 knockdown inhibited cell proliferation and induced apoptosis in vitro. **A** TCGA database indicated GTSE1 was positively associated with KIF17. **B, C** Efficiency of GTSE1 knockdown were validated in 786-O and Caki-1 cells by western blot. **D, E** GTSE1 knockdown suppresses cell growth of 786-O and Caki-1 cells, assessed by bright-field imaging (Left) and quantification (Right). **F, G** MTS assay showed that GTSE1 knockdown inhibited the cell growth in 786-O and Caki-1 cells. **H, I** The percentage of apoptotic cells dramatically increased in 786-O cells and Caki-1 cells after knockdown GTSE1 compared to control shRNA group. **J, K** Western blot was used to explore the cleaved caspase-3 and BCL-2 protein alteration after GTSE1 knockdown in 786-O and Caki-1 cells. Error bars represent SD of the mean. **p < 0.01, ***p < 0.001.

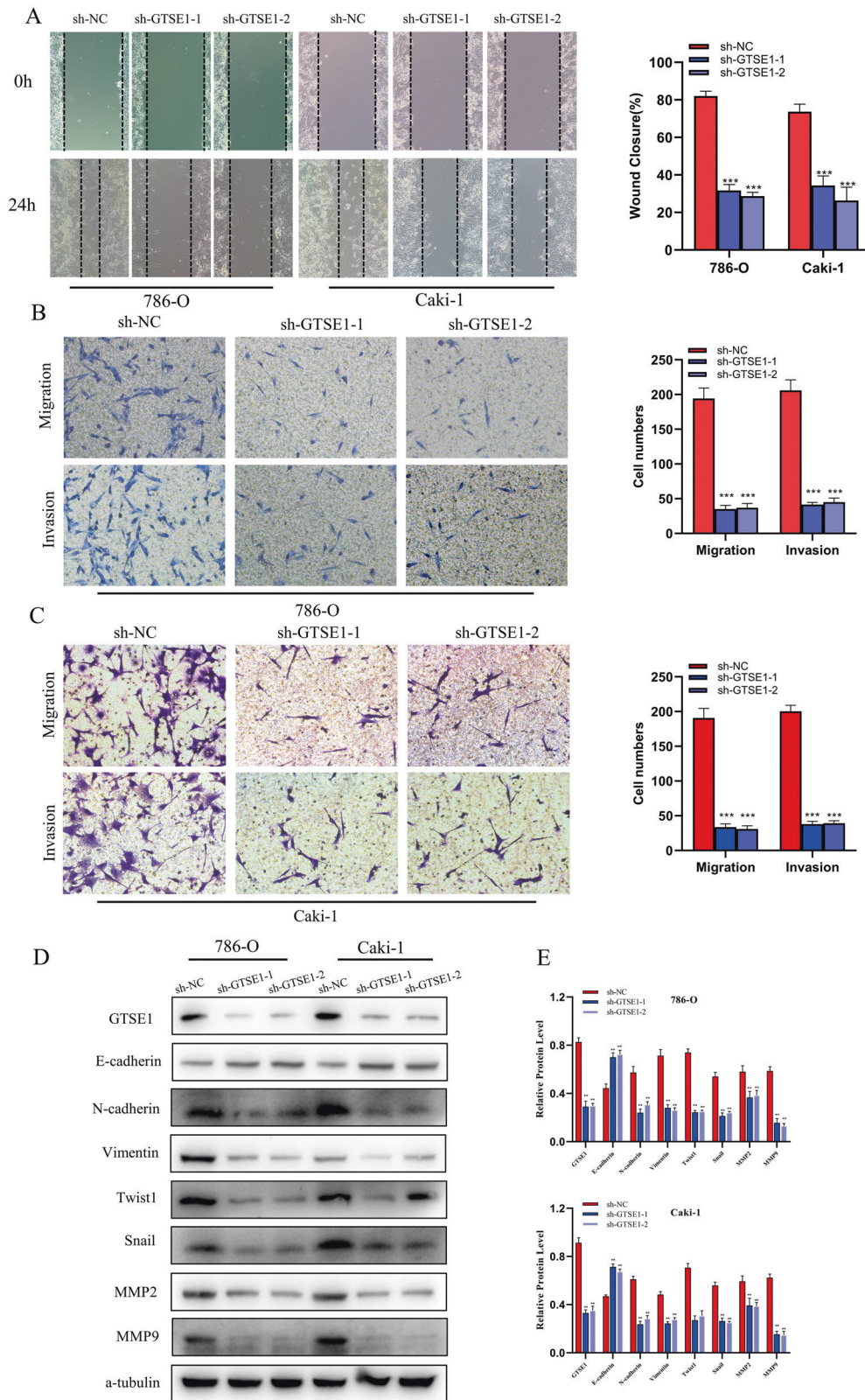


Fig. 4 GTSE1 depletion impairs ccRCC cell migration and invasion in vitro. **A** Wound-healing assay indicated that GTSE1 knockdown suppressed cell migratory ability in 786-O and Caki-1 cells. **B, C** Transwell assay indicated that GTSE1 attenuation significantly decreased migration and invasion in 786-O and Caki-1 cells. **D, E** Western blot was used to explore the epithelial mesenchymal transition (EMT)-related protein alteration after GTSE1 knockdown in 786-O and Caki-1 cells. The relative protein level of EMT-related protein (**E**). ** $p < 0.01$, *** $p < 0.001$.

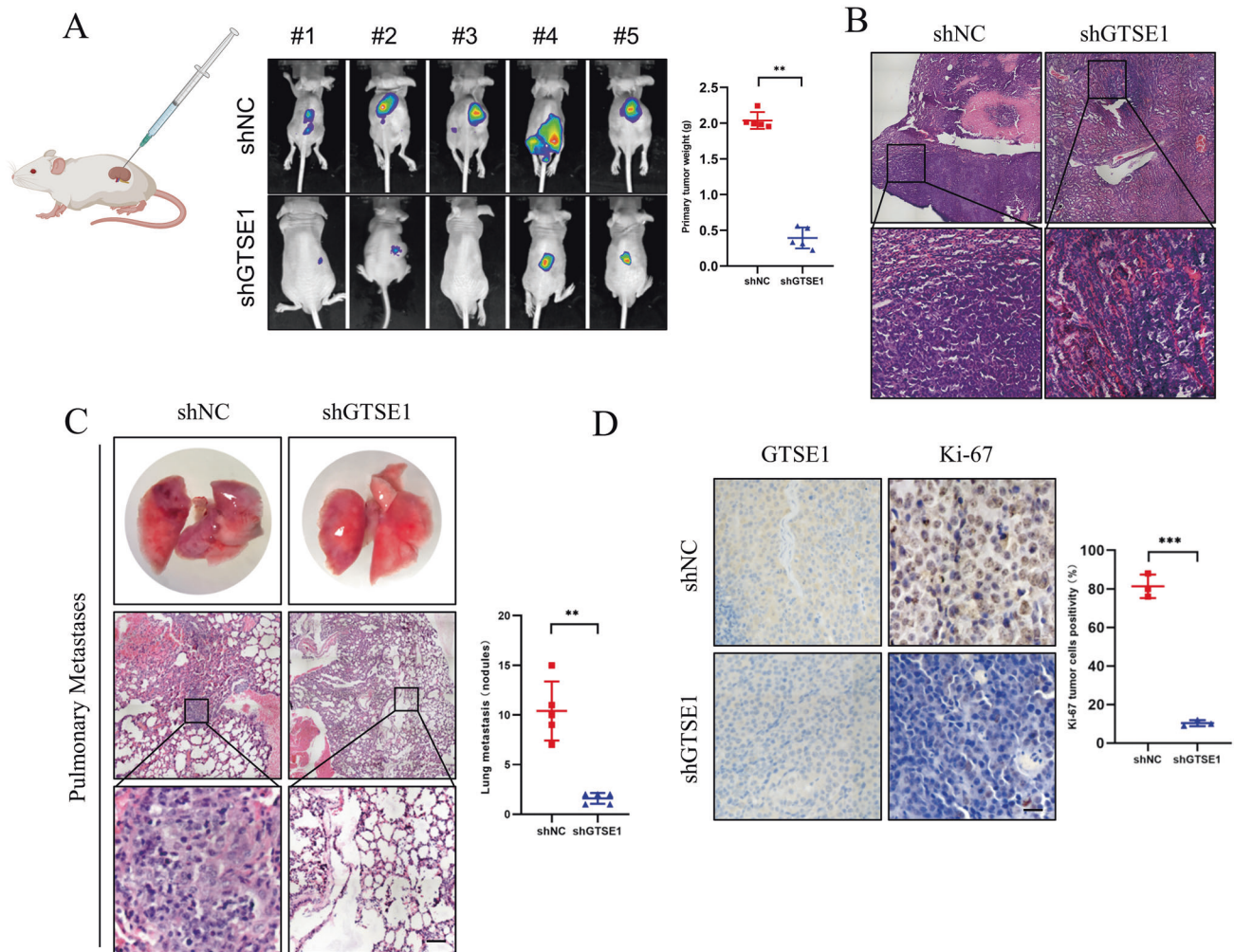


Fig. 5 GTSE1 knockdown suppresses tumor growth and metastasis in vivo. **A** (Left) Representative bioluminescent images of nude mice undergone orthotopic implantation with Luc-labeling SN12-PM6 cells stably transfected by control shRNA or shGTSE1. (Right) Tumors were resected on 4 weeks and measured. **B** Histopathological analysis of the tumors in the shGTSE1 and control group. **C** Representative hematoxylin & eosin staining of lung tissues from the different groups. **D** (Left) Representative IHC staining images of GTSE1 and Ki-67 for primary renal tumors. The scale bar represents 20 μ m. (Right) Quantitative analyses for Ki-67 positive SN12-PM6 cells stably expressing control shRNA or shGTSE1.

orthotopic tumorigenesis studies were conducted by injecting ccRCC cell lines SN12-PM6 which stably expressed luciferase and control shRNA or shGTSE1 into the right kidney of nude mice. At four weeks after injection, bioluminescent signals and orthotopic xenograft tumor weight in the GTSE1 knockdown group were significantly lower than those in the control group (Fig. 5A). Histopathological analysis of the tumors clearly showed the interface between the tumor and normal renal tissue in the shGTSE1 and control group (Fig. 5B). Consistently, the metastatic lesions of the lungs in the shGTSE1 group were also significantly reduced in comparison with those in the control group (Fig. 5C). To confirm whether the suppressed tumor growth and metastases were due to impaired proliferation induced by GTSE1 depletion, we prepared immune-stained tumors for the targeted GTSE1 and proliferation marker Ki-67. The GTSE1 knockdown was validated, and the corresponding cells with Ki-67 positivity were reduced significantly in the shGTSE1 group (Fig. 5D). Collectively, these observations demonstrated that GTSE1 knockdown significantly inhibits the growth and metastatic capacities of ccRCC cells in vivo.

GTSE1 inhibition upregulated KLF4 in ccRCC

To explore the molecular mechanism underlying the GTSE1-mediated regulation of cell proliferation and invasion, we

performed RNA sequencing (RNA-seq) analysis of Caki-1 cells after GTSE1 knockdown. The volcano plot of differentially expressed genes (DEGs) is shown in Fig. 6A. The Kyoto Encyclopedia of Genes and Genomes (KEGG) analysis of GTSE1-altered genes showed enrichment of some classic signaling pathways, including the p53 and FoxO signaling pathways (Fig. 6B). These data indicate that GTSE1 plays multiple roles in the development and progression of ccRCC cells. Interestingly, we found that Krüppel-like factor 4 (KLF4) expression was significantly upregulated in the GTSE1 knockdown group. KLF4 is a key transcription factor that plays a tumor-suppressor role in several solid tumors. In addition, our previous study also indicated that KLF4 played an important role in suppressing the growth of ccRCC²². The analysis of the ccRCC data from the TCGA database showed that GTSE1 and KLF4 levels were negatively correlated (Fig. 6C). To verify the results in the TCGA database, we detected GTSE1 and KLF4 protein expression in eight tumor tissues and paired adjacent normal tissues using western blotting. The results suggested that there was a negative correlation between the protein expression of GTSE1 and KLF4 (Supplementary Fig. 2). Therefore, KLF4 was selected for further analysis, and its upregulated expression was validated in 786-O and Caki-1 cells after the knockdown of GTSE1 by western blotting (Fig. 6D).

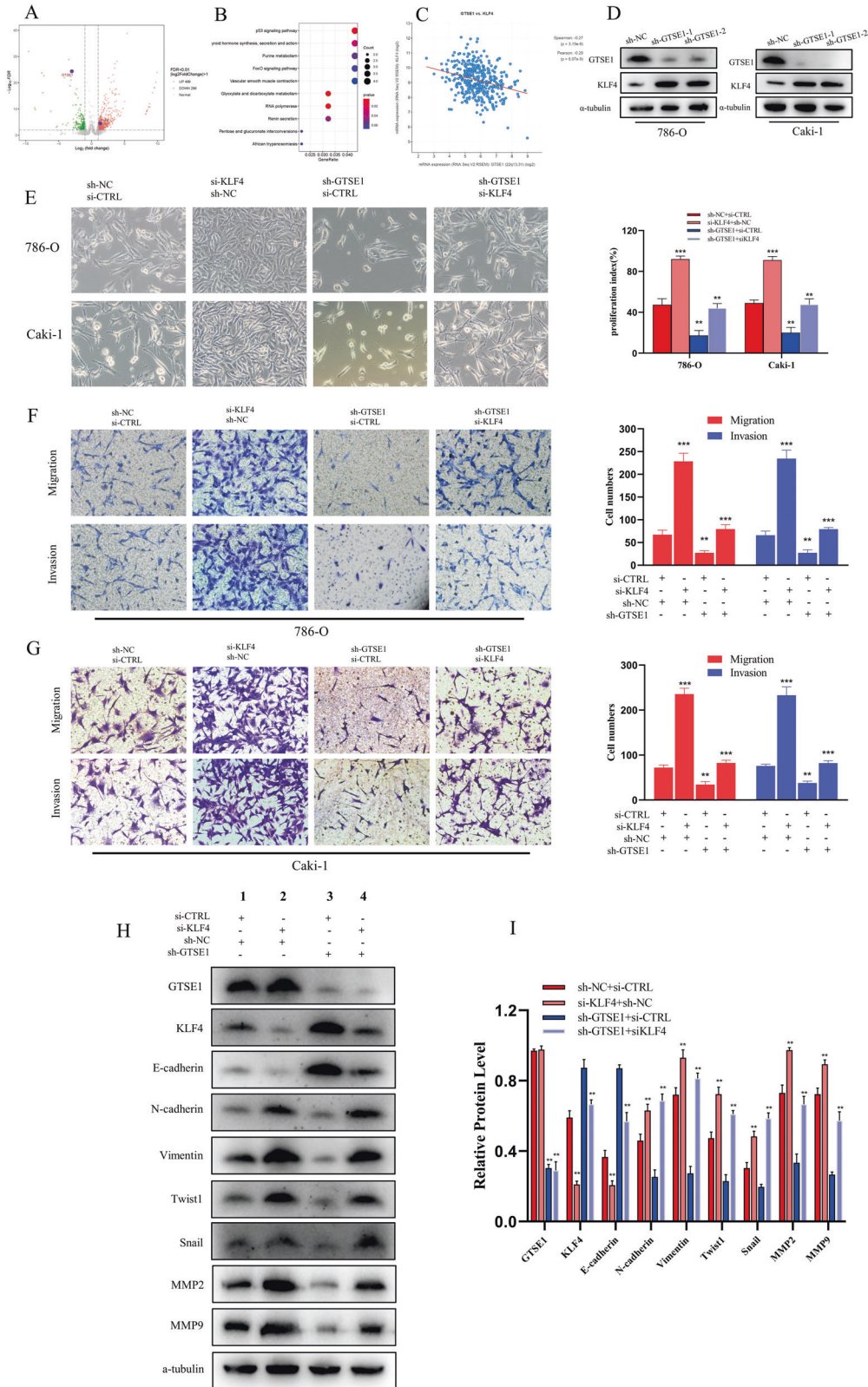


Fig. 6 GTSE1 inhibition upregulated KLF4 in ccRCC. **A** Volcano plot of differentially expressed genes (DEGs) was shown. **B** DEGs were annotated by KEGG pathway enrichment analysis. **C** TCGA database indicated GTSE1 was negatively associated with KLF4. **D** Knockdown GTSE1 upregulated KLF4 protein expression, validated by Western blot analysis in 786-O and Caki-1 cells. **E** In vitro proliferation assay was conducted in the form of rescue experiments. **F, G** In vitro transwell assay was performed in the form of rescue experiments. **H, I** Expression of the EMT-related proteins were assessed in Caki-1 Cells during the rescue assay. Graphs on the right show the quantification of western blot data from 3 independent experiments. ***p* < 0.01, ****p* < 0.001.

To illustrate whether KLF4 was critical for GTSE1-mediated ccRCC cell growth and metastasis, we inhibited KLF4 expression in 786-O and Caki-1 cells with or without GTSE1 knockdown. The results revealed that siKLF4 significantly alleviated the inhibitory effects of shGTSE1 on proliferation, migration, and invasion in ccRCC cells (Fig. 6E, F). Moreover, KLF4 was reported to be critical for the progression and maintenance of phenotypic and cellular changes associated with EMT. Therefore, we evaluated the possibility of GTSE1's contribution to EMT by KLF4. A western blot assay indicated that the EMT-related marker protein levels were partially reversed in Caki-1 shGTSE1 cells treated with siKLF4 (Fig. 6G, H).

Collectively, these results demonstrated that GTSE1 promoted the proliferation, migration and invasion abilities of ccRCC cells through inhibiting KLF4 expression.

DISCUSSION

The accumulating evidence has indicated that GTSE1 performs as oncogenic functions in many tumors^{13,14,23}. However, the exact biological role of GTSE1 in ccRCC remains obscure. In the present study, we showed that GTSE1 plays a critical role in ccRCC progression and prognosis. The analyses of the TCGA database and our own ccRCC cohorts showed that GTSE1 mRNA and protein levels were upregulated in ccRCC, especially in metastatic tissues. The increased GTSE1 expression was closely related to the tumor size and advanced stage of the ccRCC. Moreover, GTSE1 expression levels were significantly associated with shortened OS and DFS in ccRCC patients. Furthermore, knockdown regulation of GTSE1 significantly inhibited the tumor's proliferation, migration, and invasion abilities by disrupting EMT. We also found that the effects of GTSE1 as a stimulator of ccRCC progression partly depended on KLF4, which is a tumor suppressor in ccRCC. Our results showed that GTSE1 might play a proto-oncogenic role in ccRCC development and may be useful as a therapeutic target for ccRCC.

GTSE1, located in chromosome 22q13.2-q13.3, is a microtubule-localized protein that has been recently reported to be overexpressed in several solid tumors, such as prostate cancer, hepatocellular carcinoma, and bladder cancer, and its upregulation is associated with more aggressive behavior^{8,13,23,24}. Consistent with these results, our results demonstrated that GTSE1 was upregulated in ccRCC tissues and was associated with tumor size, advanced stage, and patient OS. These data strongly indicated that GTSE1 could play a crucial role in ccRCC progression. Previous studies have shown that GTSE1 silencing inhibits cell proliferation and invasion through downregulation of AKT phosphorylation and cell cycle-related proteins in HCC¹². Knockdown of GTSE1 significantly suppressed the proliferation, migration and invasion capacity in bladder cancer¹³. Consistently, our current data also showed that GTSE1 knockdown inhibited proliferation, migration, and invasion and induced apoptosis of ccRCC cells.

Chromosomal instability (CIN) is the most striking feature of human cancer, and drives tumor phenotypic switching to metastasis²⁵. CIN is also associated with poor prognosis, metastasis, and therapeutic resistance²⁶. Previous studies have also reported that GTSE1 regulates microtubule stability in mitosis by inhibiting the activity of the microtubule depolymerase MCAK. It is a key upstream regulator of chromosome alignment, spindle pole integrity and microtubule stability^{9,27}. In breast cancer, GTSE1 was identified as a microtubule-associated plus-end tracking protein required to promote cell migration through interactions with microtubule binding protein EB1²⁸. Consistently, our data showed that GTSE1 was overexpressed in ccRCC patients, especially in the metastasis group, and depletion of GTSE1 significantly suppressed the migration and invasion of ccRCC cells. Thus, these data suggest that upregulation of GTSE1 may be associated with increased metastatic potential.

This observation promoted us to further investigate the specific mechanisms of GTSE1 in migration, invasion and metastasis. Accumulating data suggests that EMT is a reversible process that leads to the loss of epithelial features and to the acquisition of a mesenchymal phenotype, and it plays an important role in tumor initiation, invasion, and metastasis^{29,30}. In hepatocellular carcinoma, GTSE1 depletion decreased the metastatic potential by affecting the EMT progression. In breast cancer and acral melanoma, GTSE1 could enhance metastasis by regulating the EMT pathway^{14,21}. Therefore, we explored EMT during the ccRCC progression. As expected, our data showed that depletion of GTSE1 in the ccRCC cell lines attenuated EMT by decreasing expression of N-cadherin, Vimentin, Twist1, Snail, MMP2 and MMP9, and increasing E-cadherin expression. Given that CD44 participates in the migration and invasion of tumors cells, and it is a marker of poor prognostic in various cancers^{31,32}. However, there was no appreciable change in the CD44 expression in the GTSE1 knockdown groups.

To better understand the contribution of GTSE1 to ccRCC progression, we performed RNA-seq analysis of Caki-1 cells with and without GTSE1 knockdown. Interestingly, we found that KLF4 expression was upregulated among the differentially expressed genes (DEGs) after GTSE1 knockdown. Mounting evidence suggests that KLF4 functions as a potent tumor suppressor in many solid tumors and plays a critical role in tumor differentiation, EMT, invasion and metastasis^{33–35}. KLF4 is also a potent tumor suppressor in hepatocellular carcinoma (HCC), and the loss of KLF4 transcriptionally downregulates Smad7 expression and leads to hyperactivation of TGF- β signaling and promotion of EMT, invasion, and metastasis of HCC cells³⁶. High matrix metalloproteinase-9 (MMP9) expression was an unfavorable prognostic biomarker for ccRCC patients³⁷. KLF4 overexpression could significantly inhibited the viability, invasion and migration of papillary thyroid cancer cells through the increased the expression of N-cadherin, MMP2 and MMP9³⁸. Our previous study also indicated that KLF4 showed low expression in ccRCC tissues and cell lines and functioned as a tumor suppressor in the development and progression of ccRCC²². In the present study, we found that GTSE1 and KLF4 were negatively correlated in the TCGA database and in eight tumor tissues and paired adjacent normal tissues. Therefore, we further explored the contribution of KLF4 in shGTSE1-mediated ccRCC cell biological function. The results showed that silencing KLF4 expression can partly rescue the downregulation of GTSE1-mediated inhibition of ccRCC progression. Moreover, siKLF4 partly rescued shGTSE1-mediated inhibition of migration by disrupting EMT molecules. Thus, upregulation of GTSE1 may facilitate tumorigenesis and progression of ccRCC by inhibiting the KLF4 expression. However, the molecular mechanism underlying the effects of GTSE1 on the expression of KLF4 needs further investigation.

In summary, our study demonstrated that GTSE1 was overexpressed in ccRCC at both mRNA and protein levels and was a poor prognostic marker. GTSE1 knockdown was found to affect cell proliferation, migration, and invasion of ccRCC cells through dysregulation of EMT. Further investigation of GTSE1 might provide potentially useful information for development of biological or pharmacological agents for ccRCC patients.

DATA AVAILABILITY

All data generated or analyzed during this study are included in this article. The datasets used and/or analyzed during the current study are available from the corresponding author on reasonable request.

REFERENCES

- Sung, H., Ferlay, J., Siegel, R. L., Laversanne, M., Soerjomataram, I., Jemal, A. et al. Global Cancer Statistics 2020: GLOBOCAN Estimates of Incidence and Mortality Worldwide for 36 Cancers in 185 Countries. *CA Cancer J Clin* **71**, 209–249 (2021).

2. Moch, H., Cubilla, A. L., Humphrey, P. A., Reuter, V. E. & Ulbright, T. M. The 2016 WHO Classification of Tumours of the Urinary System and Male Genital Organs-Part A: Renal, Penile, and Testicular Tumours. *Eur Urol* **70**, 93–105 (2016).
3. Rini, B. I., Campbell, S. C. & Escudier, B. Renal cell carcinoma. *Lancet* **373**, 1119–1132 (2009).
4. Kotecha, R. R., Motzer, R. J. & Voss, M. H. Towards individualized therapy for metastatic renal cell carcinoma. *Nat Rev Clin Oncol* **16**, 621–633 (2019).
5. Capitanio, U. & Montorsi, F. Renal cancer. *Lancet* **387**, 894–906 (2016).
6. Posadas, E. M., Limvorasak, S. & Figlin, R. A. Targeted therapies for renal cell carcinoma. *Nat Rev Nephrol* **13**, 496–511 (2017).
7. Braun, D. A., Bakouny, Z., Hirsch, L., Flippot, R., Van Allen, E. M., Wu, C. J. et al. Beyond conventional immune-checkpoint inhibition - novel immunotherapies for renal cell carcinoma. *Nat Rev Clin Oncol* **18**, 199–214 (2021).
8. Monte, M., Collavin, L., Lazarevic, D., Utrera, R., Dragani, T. A. & Schneider, C. Cloning, chromosome mapping and functional characterization of a human homologue of murine gtse-1 (B99) gene. *Gene* **254**, 229–236 (2000).
9. Tipton, A. R., Wren, J. D., Daum, J. R., Siefert, J. C. & Gorbisky, G. J. GTSE1 regulates spindle microtubule dynamics to control Aurora B kinase and Kif4A chromokinesin on chromosome arms. *J Cell Biol* **216**, 3117–3132 (2017).
10. Collavin, L., Monte, M., Verardo, R., Pflieger, C. & Schneider, C. Cell-cycle regulation of the p53-inducible gene B99. *FEBS Lett* **481**, 57–62 (2000).
11. Monte, M., Benetti, R., Collavin, L., Marchionni, L., Del Sal, G. & Schneider, C. hGTSE-1 expression stimulates cytoplasmic localization of p53. *J Biol Chem* **279**, 11744–11752 (2004).
12. Guo, L., Zhang, S., Zhang, B., Chen, W., Li, X., Zhang, W. et al. Silencing GTSE-1 expression inhibits proliferation and invasion of hepatocellular carcinoma cells. *Cell Biol Toxicol* **32**, 263–274 (2016).
13. Liu, A., Zeng, S., Lu, X., Xiong, Q., Xue, Y., Tong, L. et al. Overexpression of G2 and S phase-expressed-1 contributes to cell proliferation, migration, and invasion via regulating p53/FoxM1/CCNB1 pathway and predicts poor prognosis in bladder cancer. *Int J Biol Macromol* **123**, 322–334 (2019).
14. Xu, T., Ma, M., Chi, Z., Si, L., Sheng, X., Cui, C. et al. High G2 and S-phase expressed 1 expression promotes acral melanoma progression and correlates with poor clinical prognosis. *Cancer Sci* **109**, 1787–1798 (2018).
15. Paner, G. P., Stadler, W. M., Hansel, D. E., Montironi, R., Lin, D. W. & Amin, M. B. Updates in the Eighth Edition of the Tumor-Node-Metastasis Staging Classification for Urologic Cancers. *Eur Urol* **73**, 560–569 (2018).
16. Huang, Y., Li, W., Yan, W., Wu, J., Chen, L., Yao, X. et al. Loss of PICH promotes chromosome instability and cell death in triple-negative breast cancer. *Cell Death Dis* **10**, 428 (2019).
17. Chen, W., Niu, S., Ma, X., Zhang, P., Gao, Y., Fan, Y. et al. RhoB Acts as a Tumor Suppressor That Inhibits Malignancy of Clear Cell Renal Cell Carcinoma. *PLoS One* **11**, e0157599 (2016).
18. Yin, L., Li, W., Xu, A., Shi, H., Wang, K., Yang, H. et al. SH3BGRL2 inhibits growth and metastasis in clear cell renal cell carcinoma via activating hippo/TEAD1-Twist1 pathway. *EBioMedicine* **51**, 102596 (2020).
19. Menon, S. S., Guruvayoorappan, C., Sakthivel, K. M. & Rasmji, R. R. Ki-67 protein as a tumour proliferation marker. *Clin Chim Acta* **491**, 39–45 (2019).
20. Mani, S. A., Guo, W., Liao, M. J., Eaton, E. N., Ayyanan, A., Zhou, A. Y. et al. The epithelial-mesenchymal transition generates cells with properties of stem cells. *Cell* **133**, 704–715 (2008).
21. Lin, F., Xie, Y. J., Zhang, X. K., Huang, T. J., Xu, H. F., Mei, Y. et al. GTSE1 is involved in breast cancer progression in p53 mutation-dependent manner. *J Exp Clin Cancer Res* **38**, 152 (2019).
22. Song, E., Ma, X., Li, H., Zhang, P., Ni, D., Chen, W. et al. Attenuation of kruppel-like factor 4 facilitates carcinogenesis by inducing g1/s phase arrest in clear cell renal cell carcinoma. *PLoS One* **8**, e67758 (2013).
23. Lai, W., Zhu, W., Li, X., Han, Y., Wang, Y., Leng, Q. et al. GTSE1 promotes prostate cancer cell proliferation via the SP1/FOXM1 signaling pathway. *Lab Invest* **101**, 554–563 (2021).
24. Wu, X., Wang, H., Lian, Y., Chen, L., Gu, L., Wang, J. et al. GTSE1 promotes cell migration and invasion by regulating EMT in hepatocellular carcinoma and is associated with poor prognosis. *Sci Rep* **7**, 5129 (2017).
25. Gao, C., Su, Y., Koeman, J., Haak, E., Dykema, K., Essenberg, C. et al. Chromosome instability drives phenotypic switching to metastasis. *Proc Natl Acad Sci U S A* **113**, 14793–14798 (2016).
26. Bakhroum, S. F. & Cantley, L. C. The Multifaceted Role of Chromosomal Instability in Cancer and Its Microenvironment. *Cell* **174**, 1347–1360 (2018).
27. Bendre, S., Rondelet, A., Hall, C., Schmidt, N., Lin, Y. C., Brouhard, G. J. et al. GTSE1 tunes microtubule stability for chromosome alignment and segregation by inhibiting the microtubule depolymerase MCAK. *J Cell Biol* **215**, 631–647 (2016).
28. Scolz, M., Widlund, P. O., Piazza, S., Bublik, D. R., Reber, S., Peche, L. Y. et al. GTSE1 is a microtubule plus-end tracking protein that regulates EB1-dependent cell migration. *PLoS One* **7**, e51259 (2012).
29. Pastushenko, I. & Blanpain, C. EMT Transition States during Tumor Progression and Metastasis. *Trends Cell Biol* **29**, 212–226 (2019).
30. Mittal, V. Epithelial Mesenchymal Transition in Tumor Metastasis. *Annu Rev Pathol* **13**, 395–412 (2018).
31. Basakran, N. S. CD44 as a potential diagnostic tumor marker. *Saudi Med J* **36**, 273–279 (2015).
32. Jing, F., Kim, H. J., Kim, C. H., Kim, Y. J., Lee, J. H. & Kim, H. R. Colon cancer stem cell markers CD44 and CD133 in patients with colorectal cancer and synchronous hepatic metastases. *Int J Oncol* **46**, 1582–1588 (2015).
33. Zhao, W., Hisamuddin, I. M., Nandan, M. O., Babbin, B. A., Lamb, N. E. & Yang, V. W. Identification of Kruppel-like factor 4 as a potential tumor suppressor gene in colorectal cancer. *Oncogene* **23**, 395–402 (2004).
34. Yan, Y., Li, Z., Kong, X., Jia, Z., Zuo, X., Gagea, M. et al. KLF4-Mediated Suppression of CD44 Signaling Negatively Impacts Pancreatic Cancer Stemness and Metastasis. *Cancer Res* **76**, 2419–2431 (2016).
35. Yu, F., Li, J., Chen, H., Fu, J., Ray, S., Huang, S. et al. Kruppel-like factor 4 (KLF4) is required for maintenance of breast cancer stem cells and for cell migration and invasion. *Oncogene* **30**, 2161–2172 (2011).
36. Sun, H., Peng, Z., Tang, H., Xie, D., Jia, Z., Zhong, L. et al. Loss of KLF4 and consequential downregulation of Smad7 exacerbate oncogenic TGF-beta signaling in and promote progression of hepatocellular carcinoma. *Oncogene* **36**, 2957–2968 (2017).
37. Niu, H., Li, F., Wang, Q., Ye, Z., Chen, Q. & Lin, Y. High expression level of MMP9 is associated with poor prognosis in patients with clear cell renal carcinoma. *PeerJ* **6**, e5050 (2018).
38. Wang, Q., Xu, J., Chen, Y. & Liu, L. KLF4 overexpression decreases the viability, invasion and migration of papillary thyroid cancer cells. *Exp Ther Med* **18**, 3493–3501 (2019).

AUTHOR CONTRIBUTIONS

W.C., X.M., B.W., and X.Z. designed the study. Y.H., Y.X., T.G., D.L., and C.W. collected the data. W.C., Y.L., and H.W. performed the experiments. S.W. and W.Z. assisted with animal breeding. H.M., X.L., and H.L. assisted the bioinformatics study. W.C. and H.W. wrote the manuscript. All authors contributed to the article and approved the submitted version.

FUNDING

This work is supported by the National Natural Science Foundation of China (Grant No. 81972389, 81770790, 81802804), the Fostering Fund of Chinese PLA General Hospital for National Excellent Young Scholar Science Fund(2020-YQPY-006), the Military Young Scholar Medical Research Fund of Chinese PLA General Hospital (QNF19068) and the PLA Youth Training Project for Medical science(19QN060).

COMPETING INTERESTS

The authors declare no competing interests.

ETHICS APPROVAL

The studies involving human participants were reviewed and approved by the Ethics Committee of PLA General Hospital. The animal study was reviewed and approved by the Medical Experimental Animal Care Commission of PLA General Hospital.

ADDITIONAL INFORMATION

Supplementary information The online version contains supplementary material available at <https://doi.org/10.1038/s41374-022-00797-5>.

Correspondence and requests for materials should be addressed to Baojun Wang, Xin Ma or Xu Zhang.

Reprints and permission information is available at <http://www.nature.com/reprints>

Publisher's note Springer Nature remains neutral with regard to jurisdictional claims in published maps and institutional affiliations.